Eur. J. Mineral.
2005, **17**, 475-481

Crystal structure and chemistry of trilithionite-2M_2 and polylithionite-2M_2

MARIA FRANCA BRIGATTI[1,*], ENRICO CAPRILLI[1], DANIELE MALFERRARI[1], LUCA MEDICI[2] and LUCIANO POPPI[1]

[1]Dipartimento di Scienze della Terra dell'Università di Modena e Reggio Emilia,
Via S. Eufemia 19, I-41100 Modena, Italy
[2]CNR – Istituto di Metodologie per l'Analisi Ambientale, C.da S. Loja, I-85050 - Tito Scalo (PZ), Italy

Abstract: The crystal chemistry of three Li-bearing mica-2M_2 crystals from pegmatites has been studied by chemical analyses and single crystal X-ray diffraction; their belonging to the trilithionite-polylithionite join is highlighted by the following compositional ranges in atoms per formula unit [based on $O_{12-(x+y)}(OH)_xF_y$] : $3.198 \le Si \le 3.538$, $0.462 \le {}^{[IV]}Al \le 0.811$, $1.195 \le {}^{[VI]}Al \le 1.390$, $0.031 \le (Fe+Mn) \le 0.072$, $1.522 \le Li \le 1.757$, $0.872 \le K \le 0.906$, $0.030 \le Na \le 0.073$, $0.000 \le (Cs+Rb) \le 0.099$, $1.541 \le F \le 1.722$. The correlation between F and Li content is confirmed, as observed in Li-rich micas.

Crystal structure refinements were carried out in space group $C2/c$ (R values vary between 0.030 and 0.031). The crystal chemistry is mostly influenced by tetrahedral chemical composition. Increasing ${}^{[IV]}Al$ content, α and ψ_{M1} parameters increase; Si content involves a lowering of the interlayer separation and tetrahedral thickness. Li content affects octahedral thickness. The stability of 2M_2 polytype seems to be induced by a relative increase of Δz tetrahedral parameter, which reduces the repulsion between basal tetrahedral oxygen atoms. Unlike Li-bearing muscovite, trioctahedral Li-bearing mica crystals show an octahedral occupancy not related to octahedral charge.

Key-words: mica, trilithionite, polylithionite, lithium, 2M_2 polytype.

Introduction

The crystal structure, composition and polytypism of the micas were recently reviewed (Brigatti & Guggenheim, 2002; Ferraris & Ivaldi, 2002; Nespolo & Ďurovič, 2002). These contributions evidence the significant advancement in describing the crystal chemistry of true micas belonging to 1M polytype, mostly showing trioctahedral occupancy, and 2M_1 polytype, mostly dioctahedral. More limited results are available for 2M_2, 3T and 2O sequences both true and brittle micas.

2M_2 polytype was detected for a limited set of samples, mostly Li-containing trioctahedral micas (Takeda *et al.*, 1971; Sartori *et al.*, 1973; Guggenheim, 1981) or dioctahedral micas with uncommon interlayer composition (Zhoukhlistov *et al.*, 1973; Ni & Hughes, 1996). Trioctahedral micas-2M_2 in the system K-Li-Fe-Al-Si [Takeda *et al.*, 1971; Sartori *et al.*, 1973 and Guggenheim, 1981 ("lepidolite-2M_2" from Radkovice, Czech Republic)] as well as the dioctahedral nanpingite-2M_2 (Ni & Hughes, 1996) were refined in the space group $C2/c$ and indicate the presence of a large *trans*-site and two equivalent *cis*-sites, whereas ordering of tetrahedral cations is unusual. Unlike 1M polytype, no octahedral ordering between octahedral *cis*-sites was indicated for 2M_2 polytypic arrangement in Li-bearing micas.

At present, there are relatively few published studies on crystals belonging to the 2M_2 polytype in the K-Li-Fe-Al-Si trioctahedral mica system. Accordingly, this paper attempts to: (1) introduce three new crystal structure refinements of trioctahedral mica-2M_2 crystals with unusual composition between trilithionite and polylithionite; (2) identify the ordering pattern of the octahedral and tetrahedral sites along the trilithionite-polylithionite join; (3) compare the 2M_1 and 2M_2 long-range ordering for crystals along the Al^{3+} -Li^{+} join.

Samples

Samples under examination come from Varuträsk (Västerbotten, Sweden) and from Chèdeville (France). The sample from Varuträsk (label: SBT) is from the Varuträsk pegmatite. It is mostly made from mica species, pink in colour, with maximum crystal dimensions of 9 mm. Mica is also associated to albite and stibiotantalite, an uncommon Sb, Ta, and Nb oxide. The outcrop from Varuträsk, genetically related to the Revsunb granite (Quensel, 1955), is a complex granitic LCT pegmatite, according to the Černý nomenclature (Černý, 1992).

Samples from Chèdeville (labels: Lch 59a and Lch 132) were also selected from LCT aplitic pegmatites

*E-mail: brigatti@unimore.it

0935-1221/05/0017-0475 $ 3.15
DOI: 10.1127/0935-1221/2005/0017-0475

Table 1. Averaged chemical composition and chemical formulae for trilithionite-2M_2 and polylithionite-2M_2 crystals.

	SBT	Lch 59a	Lch132		SBT	Lch 59a	Lch132
	Chemical composition (oxide wt%)				Chemical formula (apfu) based on $O_{12-(x+y)}OH_xF_y$		
SiO_2	50.87	46.33	48.00	[iv]Si	3.538	3.189	3.293
Al_2O_3	20.21	27.14	25.53	[iv]Al	0.462	0.811	0.707
TiO_2	0.03	0.10	0.06	[iv]Total	4.000	4.000	4.000
Cr_2O_3	b.d.l	0.01	b.d.l	[vi]Al	1.195	1.390	1.357
FeO	0.29	0.44	0.15	[vi]Ti	0.001	0.005	0.003
MgO	0.06	b.d.l	b.d.l	[vi]Cr^{3+}	-	0.001	-
MnO	0.23	0.80	0.75	[vi]Fe^{2+}	0.017	0.025	0.008
Li_2O	6.28	5.50	5.70	[vi]Mg	0.006	-	-
BaO	b.d.l	0.08	b.d.l	[vi]Mn	0.014	0.047	0.044
CaO	0.03	b.d.l	0.03	[vi]Li	1.757	1.522	1.572
Na_2O	0.22	0.55	0.34	[vi]Total	2.990	2.990	2.984
Rb_2O	1.70	b.d.l	b.d.l	[xii]Ca	0.002	-	0.002
Cs_2O	0.77	b.d.l	b.d.l	[xii]Ba	-	0.002	-
K_2O	10.21	9.93	10.32	[xii]Na	0.030	0.073	0.045
H_2O	1.20	2.00	1.80	[xii]K	0.906	0.872	0.903
F	7.83	7.08	7.32	[xii]Cs	0.023	-	-
Cl	b.d.l	0.01	b.d.l	[xii]Rb	0.076	-	-
Totale	99.93	99.97	100.00	[xii]Total	1.037	0.947	0.950
				OH	0.278	0.459	0.412
				F	1.722	1.541	1.588
				O	10.000	10.000	10.000

Note: b.d.t. = below detection threshold.

(Raimbault, 1998) outcropping in the French Central Massive. Chèdeville pegmatite is related to the Saint-Sylvestre granite and is formed by a complex and stratified veins. Chèdeville complex also hosts metasomatic units, rich in Li-rich trioctahedral micas. Sample Lch 59a and Lch 132 occurred in veins located in the main complex body, distant approximately 200 m one from the other. Micas in both samples are associated to albite, quartz and K-feldspar. Mica from sample Lch 132 is pink-violet in colour with crystals approximately 1 mm in dimensions, whereas mica from sample Lch 59a is silver grey, with crystals approximately 0.1 mm in dimensions.

Experimental methods

Electron-microprobe analysis and normalization of the formula unit

Chemical compositions for crystals and crystal portions used in structure refinement (Table 1) were obtained by energy dispersive and wavelength dispersive methods (ARL-SEMQ equipped with Tracor Northern EDS apparatus. Operating conditions were: accelerating voltage 15 kV, sample current 15 nA, and beam diameter 5 μm). In each crystal, several spots were analyzed to check for sample homogeneity. The F content was determined by the method reported by Foley (1989). No evidence of volatilization of F was observed. Analysis and data reduction were performed using the Probe software package of Donovan (1995). Lithium and OH determinations were done on homogeneous portions carefully selected from the same sample used to provide the crystal refined. Lithium determinations were performed by inductively coupled plasma atomic-emission spectrometry (ICP-AES, Varian Liberty 200). Twenty-five mg of each sample were digested with a mixture of HF (62 %) and HNO_3 (38 %) in closed Teflon crucibles in a microwave. The OH content was obtained by means of Seiko SSC 5200 thermogravimetric analysis (TG) equipped with a mass spectrometer (ESS, GeneSys Quadstar 422). A sample of about 2-3 mg of powder was heated at a rate of 10°C/min in Ar gas (flow rate 30mL/min). Chemical compositions reported in Table 1 were obtained by combining the above results. The chemical formula (Table 1) was based on $O_{12-(x+y)}(OH)_xF_y$.

Collection of X-ray-diffraction data

Crystals selected for X-ray data collection (labels: SBT, Lch 59a, and Lch 132) show a monoclinic cell (space group $C2/c$). All the crystals exhibited sharp reflections without the streaking commonly indicative of stacking disorder. Each crystal was mounted onto a Siemens P4P rotating-anode fully automated four-circle diffractometer with graphite-monochromatized Mo$K\alpha$ radiation (λ = 0.71073 Å, 50 kV, 140 mA) equipped with XSCANS software (Siemens, 1996). The unit-cell parameters, refined on about 100 medium angle reflections are reported in Table 2. Intensities for reflections + h, ± k, ± l were collected at $2\theta \leq$ 70.0° using the ω scan mode (window width from 1.8 to

Table 2. Details on the data collection and structure refinement of the mica-2M_2 crystals (space group $C2/c$): crystal size, number of unique reflections (N), structure refinement agreement factor (R_{obs}), and unit-cell parameters (number in parentheses: standard deviation).

Samples	Crystal dimension (mm)	N	R	Unit-cell parameters				
				a (Å)	b (Å)	c (Å)	β (°)	V (Å^3)
SBT	0.28 × 0.28 × 0.07	1410	0.030	9.029(4)	5.203(1)	20.201(6)	99.35(3)	936.4(4)
Lch 59a	0.16 × 0.10 × 0.08	1025	0.030	9.056(3)	5.216(2)	20.282(5)	99.64(2)	944.5(5)
Lch 132	0.16 × 0.10 × 0.09	1323	0.031	9.033(3)	5.210(3)	20.271(5)	99.71(2)	940.3(5)

4.0°), with scan speeds inversely proportional to intensity, varying from 1 to 5°/minute. The intensity data were then corrected for Lorentz-polarization and absorption effects (North *et al*., 1968). The structure refinements were performed in the space group $C2/c$ using the least-squares refinement "SHELX –97" program package (Sheldrick, 1997) on reflections with $I \geq 3\sigma(I)$. Atomic-position parameters from Guggenheim (1981) were used as initial values for all refinements. Scattering factor curves were calculated using the method of Sales (1987) and the tables of Cromer & Mann (1968) assuming full-ionization of octahedral M and interlayer A atoms and half-ionization for oxygen atoms and cations in tetrahedral sites. In the final cycles, anisotropic displacement parameters for T, M, K and O were refined. The final refinement yielded the following agreement factors: sample SBT = 0.030; sample Lch 59a = 0.030; sample Lch 132 = 0.031. A final calculated difference electron density (DED) map does not reveal a significant excess in electron density above background. Table 3 lists atom coordinates and equivalent

Table 3. Atom coordinates and equivalent isotropic and anisotropic displacement factors (Å^2) for the crystals of trilithionite-2M_2 and polylithionite-2M_2.

Atom	x/a	y/b	z/c	Ueq	U11*	U22*	U33*	U23*	U13*	U12*
					Sample SBT					
O1	0.0917(2)	0.5740(3)	0.05306(6)	0.0188(2)	0.0240(7)	0.0198(6)	0.0122(5)	-0.0004(5)	0.0019(4)	-0.0055(5)
O2	0.2682(2)	0.1056(3)	0.05302(6)	0.0190(3)	0.0256(7)	0.0186(6)	0.0120(5)	0.0011(5)	0.0011(5)	-0.0043(5)
O3	0.2089(2)	0.3254(3)	0.16633(7)	0.0213(3)	0.0257(7)	0.0179(6)	0.0201(7)	0.0011(5)	0.0029(5)	0.0070(5)
O4	0.4721(2)	0.1151(3)	0.16605(7)	0.0217(3)	0.0144(6)	0.0317(8)	0.0190(6)	-0.0029(6)	0.0021(5)	0.0003(5)
O5	0.2343(2)	0.8239(3)	0.16250(7)	0.0218(4)	0.0249(7)	0.0197(6)	0.0194(6)	0.0016(5)	-0.0002(5)	-0.0067(5)
F	0.9466(2)	0.0718(4)	0.04958(6)	0.0413(6)	0.0326(8)	0.073(1)	0.0191(6)	0.0011(7)	0.0051(5)	0.0282(8)
T1	0.12540(5)	0.58624(9)	0.13373(2)	0.0100(1)	0.0092(2)	0.0090(2)	0.0119(2)	0.0001(2)	0.0019(1)	-0.0005(2)
T2	0.29388(5)	0.0916(1)	0.13370(2)	0.0105(1)	0.0101(2)	0.0103(2)	0.0113(2)	-0.0004(2)	0.0020(1)	0.0000(2)
M1	0.25	0.75	0	0.023(1)	0.023(2)	0.023(2)	0.022(2)	-0.004(2)	0.001(2)	0.006(2)
M2	0.08564(9)	0.2580(2)	0.00013(4)	0.0121(2)	0.0121(3)	0.0130(3)	0.0113(3)	0.0005(3)	0.0017(2)	0.0012(3)
A	0	0.0900(1)	0.25	0.0242(2)	0.0234(3)	0.0242(3)	0.0247(3)	0	0.0026(2)	0
					Sample Lch 59a					
O1	0.0885(2)	0.5708(3)	0.05271(6)	0.0186(4)	0.0192(8)	0.0213(10)	0.0150(6)	0.0007(7)	0.0016(5)	0.0024(8)
O2	0.2684(2)	0.1115(3)	0.05309(6)	0.0202(5)	0.0223(8)	0.0224(9)	0.0151(6)	0.0001(7)	0.0011(5)	-0.0014(8)
O3	0.2033(2)	0.3192(3)	0.16694(7)	0.0227(5)	0.0284(10)	0.0195(10)	0.0213(7)	0.0005(6)	0.0077(7)	0.0068(8)
O4	0.4733(2)	0.1302(3)	0.16629(7)	0.0276(5)	0.0189(8)	0.0378(12)	0.0257(7)	-0.0034(8)	0.0025(6)	-0.0008(8)
O5	0.2434(2)	0.8199(3)	0.16143(7)	0.0235(5)	0.0244(9)	0.0196(10)	0.0249(8)	0.0035(6)	-0.0008(6)	-0.0047(7)
F	0.9491(2)	0.0699(3)	0.04940(6)	0.0313(5)	0.0296(8)	0.0438(11)	0.0212(6)	-0.0004(7)	0.0062(5)	0.0137(8)
T1	0.12577(6)	0.5861(1)	0.13434(2)	0.0134(2)	0.0139(3)	0.0123(3)	0.0140(3)	0.0001(2)	0.0021(2)	0.0018(3)
T2	0.29499(6)	0.0933(1)	0.13432(2)	0.0125(2)	0.0115(3)	0.0133(3)	0.0133(3)	0.0000(2)	0.0036(2)	0.0013(3)
M1	0.25	0.75	0	0.027(2)	0.020(3)	0.034(4)	0.028(3)	-0.006(2)	0.006(2)	0.011(3)
M2	0.08478(9)	0.2548(2)	0.00005(3)	0.0135(2)	0.0138(4)	0.0122(4)	0.0150(3)	0.0010(3)	0.0038(3)	0.0000(3)
A	0	0.0929(2)	0.25	0.0289(2)	0.0287(4)	0.0289(5)	0.0290(3)	0	0.0041(3)	0
					Sample Lch 132					
O1	0.0872(2)	0.5698(3)	0.05290(6)	0.0188(4)	0.0229(7)	0.0188(7)	0.0140(6)	-0.0019(5)	0.0009(5)	-0.0003(6)
O2	0.2681(2)	0.1152(3)	0.05297(6)	0.0189(4)	0.0179(6)	0.0235(8)	0.0148(6)	0.0009(5)	0.0016(4)	-0.0015(6)
O3	0.2034(2)	0.3199(3)	0.16710(7)	0.0226(4)	0.0277(8)	0.0198(7)	0.0201(7)	0.0012(6)	0.0034(6)	0.0099(6)
O4	0.4730(2)	0.1301(3)	0.16689(7)	0.0217(4)	0.0112(6)	0.034(1)	0.0195(7)	0.0002(6)	0.0022(5)	-0.0014(6)
O5	0.2432(2)	0.8163(3)	0.16081(7)	0.0239(4)	0.0257(8)	0.0212(8)	0.0223(7)	0.0044(6)	-0.0028(6)	-0.0056(6)
F	0.9502(2)	0.0675(3)	0.04946(6)	0.0293(5)	0.0249(7)	0.044(1)	0.0195(6)	-0.0017(6)	0.0037(5)	0.0100(7)
T1	0.12582(5)	0.5869(1)	0.13437(2)	0.0105(2)	0.0086(2)	0.0095(2)	0.0131(2)	-0.0003(2)	0.0009(2)	0.0006(2)
T2	0.29486(5)	0.0950(1)	0.13441(2)	0.0107(2)	0.0091(2)	0.0097(2)	0.0132(2)	0.0003(2)	0.0015(2)	0.0006(2)
M1	0.25	0.75	0	0.028(2)	0.024(3)	0.033(3)	0.029(3)	-0.011(2)	0.005(2)	0.000(2)
M2	0.08495(7)	0.2550(2)	0.00002(3)	0.0111(2)	0.0095(3)	0.0114(3)	0.0121(3)	0.0000(2)	0.0010(2)	0.0018(2)
A	0	0.0930(2)	0.25	0.0289(2)	0.0243(3)	0.0255(3)	0.0270(3)	0	0.0019(2)	0

Table 4. Selected interatomic distances (Å) derived from structure refinement of trilithionite-2M_2 and polylithionite-2M_2 crystals.

		SBT	Lch 59a	Lch 132
T1	T1-O1	1.610(1)	1.635(2)	1.632(1)
	T1-O3	1.638(2)	1.647(2)	1.646(2)
	T1-O4	1.631(2)	1.637(2)	1.643(2)
	T1-O5	1.627(2)	1.651(2)	1.627(2)
	⟨T1-O⟩	1.626	1.642	1.637
T2	T2-O2	1.610(1)	1.627(1)	1.631(1)
	T2-O3	1.633(2)	1.643(2)	1.637(2)
	T2-O4	1.640(2)	1.648(2)	1.642(2)
	T2-O5	1.634(2)	1.625(2)	1.642(2)
	⟨T2-O⟩	1.629	1.636	1.638
M1	M1-O1(× 2)	2.128(2)	2.163(2)	2.174(2)
	M1-O2 (× 2)	2.131(1)	2.164(2)	2.177(2)
	M1-F (× 2)	2.106(2)	2.129(1)	2.137(2)
	⟨M1-O⟩	2.122	2.152	2.163
M2	M2-O1	1.957(2)	1.961(2)	1.957(2)
	M2-O1'	1.981(2)	1.968(2)	1.959(2)
	M2-O2	1.965(2)	1.970(2)	1.954(2)
	M2-O2'	1.979(2)	1.974(2)	1.963(2)
	M2-F	1.980(2)	1.963(2)	1.955(2)
	M2-F'	1.986(2)	1.966(2)	1.963(2)
	⟨M2-O⟩	1.975	1.967	1.958
A	A-O3	2.991(2)	2.943(2)	2.939(2)
	A-O3'	3.197(2)	3.252(2)	3.242(2)
	A-O4	2.984(2)	2.937(2)	2.928(2)
	A-O4'	3.204(2)	3.265(2)	3.254(2)
	A-O5	2.997(2)	2.938(2)	2.931(2)
	A-O5'	3.276(2)	3.382(2)	3.392(2)
	A-F	4.000(3)	4.019(2)	4.016(2)
	⟨A-O⟩"inner"	2.991	2.939	2.933
	⟨A-O⟩"outer"	3.226	3.300	3.296

Number in parentheses: standard deviation.

isotropic and anisotropic displacement factors whereas Table 4 reports relevant cation-anion bond lengths. Table 5 reports the mean electron count at octahedral and interlayer sites and compares data obtained from crystal structure refinement with those derived from electron microprobe analysis; Table 6 lists selected parameters derived from structure refinement. The observed and calculated structure factors are available from the autors or through the Editorial Office of EJM-Paris.

Table 5. Mean electron count (e^-) at octahedral and interlayer sites as determined by X-ray diffraction structure refinement (Xref) and by chemical data (CD).

	SBT	lch59a	lch132
Octahedral sites			
M1 (Xref)	3.22	3.01	3.11
M2 (Xref)	9.09	10.78	10.18
M1+2×M2 (Xref)	21.40	24.57	23.47
M1+2×M2 (CD)	21.69	24.59	24.72
Interlayer site			
A (Xref)	21.20	17.31	17.94
A (CD)	21.65	17.49	17.70

Table 6. Selected parameters obtained from structure refinement of trilithionite-2M_2 and polylithionite-2M_2 crystals.

	SBT	Lch 59a	Lch 132
Tetrahedral parameters			
α (°)	5.3	8.1	8.2
Δz (Å)	0.0763	0.1102	0.1257
τ_{T1}	112.4	111.9	111.9
τ_{T2}	112.4	111.8	111.9
Octahedral parameters			
ψ_{M1} (°)	60.8	61.3	61.4
ψ_{M2} (°)	58.4	58.3	58.1
Sheet thickness (Å)			
tetrahedral	2.254	2.263	2.261
octahedral	2.069	2.069	2.069
Interlayer separation	3.390	3.404	3.399

Note: α (tetrahedral rotation angle) = $\Sigma_{i=1}^{6} \alpha_i/6$ where $\alpha_i = |120° - \phi_i|/2$ and where ϕ_i is the angle between basal edges of neighboring tetrahedra articulated in the ring. Δz = [$Z_{(Obasal)max}$ - $Z_{(Obasal)min}$] [csinβ]. τ (tetrahedral flattening angle) = $\sum_{i=1}^{3}(O_{basal}\text{-}\hat{T}\text{-}O_{basal})_i/3$. ψ (octahedral flattening angle) = $\cos^{-1}$ [octahedral thickness / (2<M-O>)] (Donnay *et al*., 1964).

Results and discussion

Average chemical composition for micas 2M_2 considered is introduced in Fig. 1, as compared with other micas in the composition space K-Li-Fe-Al-Si. Sample SBT can be considered as intermediate in composition between trilithionite and polylithionite, whereas samples Lch 59a and Lch 132 are close to trilithionite in composition. For all the samples considered, the annite and siderophyllite components are very limited. As evidenced by Table 1, all the samples considered are characterized by F for OH substitutions. Moreover F and Li content are strictly related together, as common in Li-rich micas (Monier & Robert, 1986; Charoy *et al.*, 1995). Furthermore Si content increases from trilithionite to polylithionite following the exchange vector $Si_2Al_{-2}Al_{-1}Li$. An opposite trend was found for Mn, which, even if present in limited amount, decreases when Li content increases.

SBT, Lch 59a and Lch 132 crystals are meso-octahedral, with M1 much greater than the two symmetrically equivalent M2 sites (Ďurovič, 1994). Sample SBT (*i.e*., the sample with intermediate composition between trilithionite and polylithionite) when compared to trilithionite samples (*i.e*. samples Lch 59a and Lch 132) shows the lowest α angle and the smallest dimensional inequalities between octahedral sites, with the smallest ⟨M1-O⟩ distance and the greatest ⟨M2-O⟩ distance, the smallest ψ_{M1} angle and the greatest ψ_{M2}. The smallest dimensional inequality between M1 and M2 octahedra also accounts for the smallest tetrahedral basal plane corrugation as determined by Δz parameter. The interlayer separation and the tetrahedral thickness,

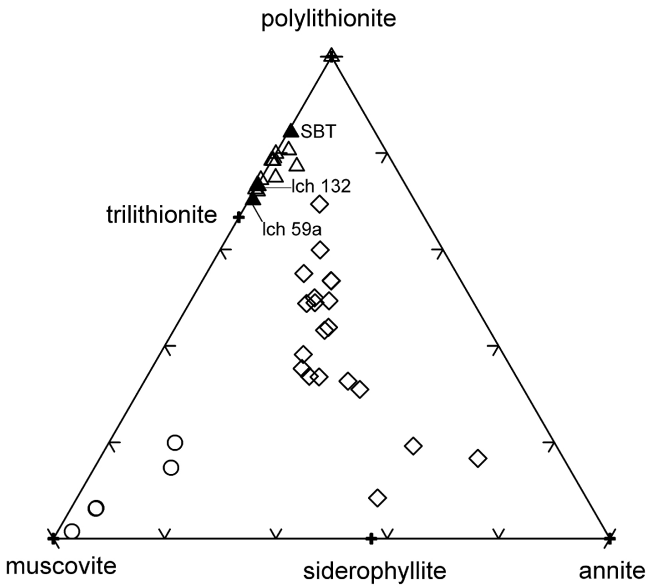

Fig. 1. Lithium-bearing micas reported on muscovite-polylithionite-annite diagram. Triangles: filled = trilithionite-2M_2 and polylithionite-2M_2 crystals from this study, open = trilithionite and polylithionite (1M, 2M_1, 2M_2 and 3T polytype) from literature (Takeda & Burnham, 1969; Sartori *et al.*, 1973; Sartori, 1976, 1977; Guggenheim, 1981; Swanson & Bailey, 1981; Backhaus, 1983); diamond = Fe-polylithionite and siderophyllite crystals from literature (Guggenheim & Bailey, 1977; Brown 1978; Weiss *et al*., 1993; Rieder *et al*., 1996; Brigatti *et al.*, 2000); circles = dioctahedral lithium-rich micas (Brigatti *et al*., 2001). Crosses: end-member compositions.

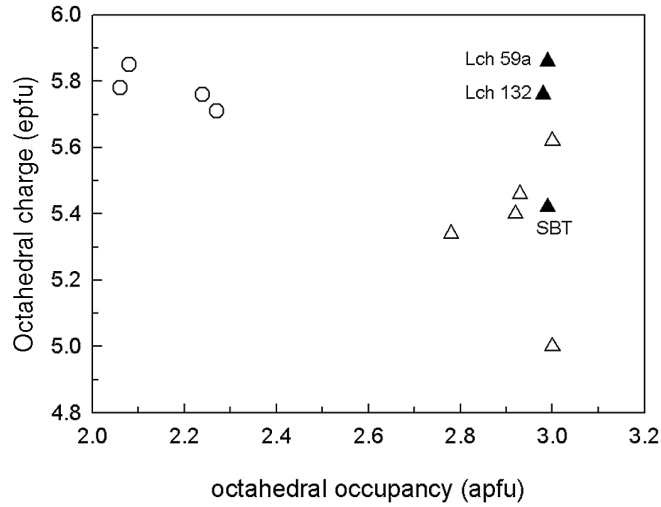

Fig. 2. Octahedral charge vs. octahedral occupancy for lithium-bearing micas along muscovite-polylithionite edge. Triangles: filled = trilithionite-2M_2 and polylithionite-2M_2 crystals from this study, open = trilithionite and polylithionite (1M, 2M_1 and 2M_2 polytype) from literature (Takeda & Burnham, 1969; Sartori et al., 1973; Sartori, 1976, 1977; Guggenheim, 1981; Swanson & Bailey, 1981); circles = dioctahedral lithium-rich micas (Brigatti *et al*., 2001).

being the smallest in SBT sample, reflect the greater Si content.

Different exchange vectors were identified for samples along the Al – Li edge of the muscovite-polylithionite-annite triangular diagram (Fig. 1).

Figure 2 reports octahedral charge *vs*. octahedral occupancy. Different trends can be observed for trioctahedral and dioctahedral crystals. In Li-bearing muscovite, the increase in octahedral occupancy is associated to a decrease in octahedral charge, thus hinting to a complex substitution mechanism involving both Li for Al and Li for vacancy substitutions. The decrease in octahedral charge following from this substitution is compensated by tetrahedral Si for Al substitution. In trioctahedral crystals considered in Fig. 2, the octahedral occupancy is always close to its theoretical value. Heterovalent octahedral substitutions involving Li are thus charge balanced in the tetrahedral sheet without appreciably affecting octahedral occupancy. In other words a lack of continuity was observed between dioctahedral and trioctahedral samples, as further enhanced by the sometime opposite crystal chemical trends. In trioctahedral samples a predominant crystal chemical role is played by tetrahedral chemical composition. When $^{[iv]}$Al increases, α increases also, thus hinting to a relatively stiff octahedral site. The tetrahedral dimensional lateral variation following from $^{[iv]}$Al substitutions can thus be compensated mostly by a distortion of the tetrahedral sheet. An increase in $^{[iv]}$Al is also associated to an increase in ψ_{M1}. A similar trend was observed for $\Delta\langle$M-O$\rangle$ also ($\Delta\langle$M-O$\rangle$ = $\langle$M1-O$\rangle$ - $\langle$M2-O$\rangle$). An increase in $^{[iv]}$Al, which is also directly related to $^{[vi]}$Al, following the substitution mechanism introducing $^{[iv]}$Al in the tetrahedral sheet (*e.g.* $^{[iv]}Si_{-2}{}^{[iv]}Al_2$ $^{[vi]}Li_{-1}{}^{[vi]}Al$), is thus significantly affecting the geometry of the octahedral site also, mostly for what concerns its distortion. The distortion of the octahedral site thus mirrors octahedral chemical substitutions and can evidence ordering patterns. $^{[iv]}$Al appears to be correlated to other octahedral cations than $^{[vi]}$Al when present. It is finally worth nothing that an increase in $^{[iv]}$Al is also associated to an increase of Na in interlayer position. This evidence could be ascribed to a secondary substitution mechanism involving the interlayer cation trying to affect octahedral lateral mean dimensions.

Li was found to affect octahedral dimensions along [001]. An increase in Li is thus associated to an increase in octahedral thickness.

Different crystal chemical trends were observed for Li-rich muscovite crystals. As introduced by Brigatti *et al.* (2001), Li which shows a good correlation with $^{[iv]}$Al, is the main chemical parameter reflected by crystal structure parameters. Most of the correlations found for trioctahedral samples, when considering $^{[iv]}$Al, apply for Li-rich muscovite crystals also, but showing a different slope (Fig. 3). The structure of both trioctahedral and dioctahedral Li-rich samples can thus be described starting from tetrahedral chemical composition, which is affected by heterovalent octahedral substitutions, even if the different structural arrangement accounts for a different behaviour.

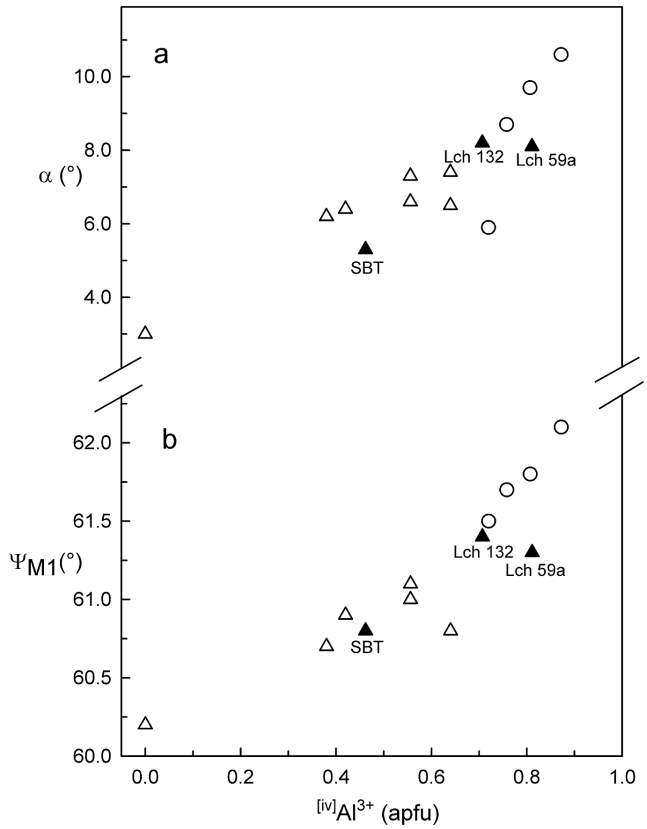

Fig. 3. (a) α *vs*. tetrahedral Al content and (b) ψ_{M1} vs. tetrahedral Al content. Symbols and samples as in Fig. 2.

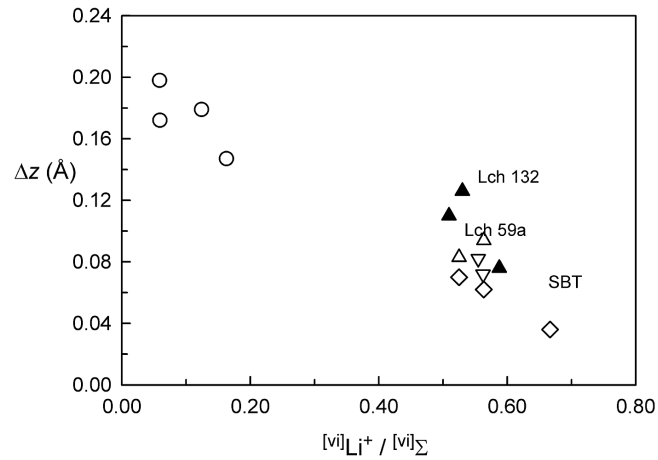

Fig. 4. Δ*z* *vs*. Li octahedral occupancy, calculated as Li over the sum of octahedral cations. Samples as in Fig. 2. Filled symbols: samples from this study; open symbols: samples from the literature. Triangles up: trilithionite-2M_2 and polylithionite-2M_2; triangles down: trilithionite-2M_1; diamonds: trilithionite-1*M* and polylithionite-1*M*; circles: Li-bearing muscovite-2M_1.

Most trioctahedral micas in the trilithionite-polylithionite join show the 2M_2 stacking.

Following Backhaus & Ďurovič (1984), micas belonging to 2M_2 polytype join the subfamily B. Unlike most of the micas, which belong to subfamily A (1*M*, 2M_1 and 3*T*) and where the coordination polyhedron for the interlayer cation is a trigonal antiprism, subfamily B shows a trigonal prism as coordination polyhedron for the interlayer cation. Thus, according to Bailey (1984), the 2M_2 polytype yields an atomic arrangement in which three basal oxygen atoms from one layer directly superimpose to three basal oxygen atoms of the layer below, leading to an energetic unfavorable arrangement relative to 2M_1 polytype. Moreover according to Appelo (1978) and Ferraris & Ivaldi (2002), Δ*z* may contribute to render 2M_2 polytype more stable. Ni & Hughes (1996) related the 2M_2 polytype stability both to interlayer substitution and high interlayer separation which reduces the repulsion between basal tetrahedral oxygen atoms. Only a few trilithionite crystals were refined in 2M_1 polytype. Those latter are characterized by a slightly minor tetrahedral Al content than 2M_2 trilithionite and polylithionite, thus also leading to an averagely lower Δ*z* and difference between octahedral site sizes. Figure 4 reports, for all the samples considered Δ*z* *vs*. Li octahedral occupancy, calculated as Li over the sum of octahedral cations. As it can be inferred from Fig. 4, different polytypes can be observed when Li occupancy is greater than 0.5. At equal Li occupancy, Δ*z* is lower for 1*M* crystals. Intermediate Δ*z* values are reached both by 2M_1 and 2M_2 samples, whereas when Δ*z* further increases 2M_2 polytype seems to be preferred. Those evidences, which agree with the theoretical assumptions introduced before, can contribute to better focus the crystal structure of Li-rich micas, even if more data is required to gain a deeper confidence and understanding on this complex subject.

Concluding remarks

This work contributes to the characterization of Li-bearing micas, with composition both close to muscovite and between trilithionite and polylithionite. Tetrahedral composition appeared to be the unifying chemical parameter for the description of both trioctahedral and dioctahedral samples, even if the crystal chemical trends, involving [iv]Al, are different between trioctahedral and dioctahedral micas and a lack of continuity was identified when considering octahedral occupancy (no sample was identified with octahedral occupancy in the range 2.3-2.8).

All the new refinements introduced in this work belong to 2M_2 polytype. Even if differences in sheet and layer topology are limited when compared to other polytypes, samples with 2M_2 polytype are characterized by a greater Δ*z*. This work confirm previous knowledge and relates it to [iv]Al content also.

Acknowledgments: This work was supported by Ministero dell'Università e della Ricerca Scientifica of Italy and by Consiglio Nazionale delle Ricerche (CNR) of Italy. Centro Interdipartimentale Grandi Strumenti (CIGS) of the University of Modena and Reggio Emilia is acknowledged for the use of the single-crystal diffractometer. We are thankful to Dr. Raimbault L. (Ecole de Mines Paris, France) for providing samples and for help in defining

genetical features of Li-rich micas from Massif Central (France). We are thankful to two unknown referees for their comments and suggestions.

References

Appelo, C.A.J. (1978): Layer deformation and crystal energy of micas and related minerals. I structural models for 1*M* and 2M_1 polytypes. *Am. Mineral.*, **63**, 782-792.

Bailey, S.W. (1984): Crystal chemistry of the true micas. *Rev. Mineral.*, **13**, S.W. Bailey Editor, 13- 60.

Backhaus, K.O. (1983): Structure refinement of a lepidolite-1*M*. *Cryst. Res. Technol.*, **18**, 1253-1260.

Backhaus, K.O. & Ďurovič, S. (1984): Polytypism of micas. I. MDO polytypes and their derivation. *Clays Clay Miner.*, **32**, 453-463.

Brigatti, M.F. & Guggenheim, S. (2002): Micas crystal chemistry and metamorphic petrology. *Rev. Mineral. Geochem.*, A. Mottana, F.P. Sassi, J.B. Thompson, S. Guggenheim editors, **46**, 1-100.

Brigatti, M.F., Lugli, C., Poppi, L., Foord, E.E., Kile, D.E. (2000): Crystal chemical variations in Li- and Fe-rich micas from Pikes Peak Batholith (central Colorado). *Am. Mineral.*, **85**, 1275-1286.

Brigatti, M.F., Kile, D.E., Poppi, M. (2001): Crystal structure and crystal chemistry of lithium-bearing muscovite-2M_1. *Can. Mineral.*, **39**, 1171-1180.

Brown, B.E. (1978): The crystal structure of 3*T* lepidolite. *Am. Mineral.*, **63**, 332-336.

Černý, P. (1992): Geochemical and petrogenetic features of mineralization in rare-element granitic pegmatites in the light of current research. *Appl. Geochem.*, **7**, 393-416.

Charoy, B., Chaussidon, M., Noronha, F. (1995): Lithium zonation in white micas from the Argemela microgranite (central Portugal): an *in-situ* ion-, electron-microprobe and spectroscopic investigation. *Eur. J. Mineral.*, **7**, 335-352.

Cromer, D.T. & Mann, J.B. (1968): X-ray scattering factors computed from numerical Hartree-Fock wave functions. *Acta Cryst.*, **A24**, 321-324.

Donnay, G., Morimoto, N., Takeda, H., Donnay, D.H. (1964): Trioctahedral one-layer micas:1. Crystal structure of a synthetic iron mica. *Acta Cryst.*, **A17**, 1369-1373.

Donovan, J.J. (1995): PROBE: PC-based data acquisition and processing for electron microprobes. *Adv. Microbeam*, 4217 King Graves Rd., Vienna, Ohio, 44473.

Ďurovič, S. (1994): Classification of phyllosilicates according to the symmetry of their octahedral sheets. *Ceramics – Silikáty*, **38**, 81-84.

Ferraris, G. & Ivaldi, G. (2002): Structural features of micas. *Rev. Mineral. Geochem.*, A. Mottana, F.P. Sassi, J.B. Thompson, S. Guggenheim editors, **46**, 117-153.

Foley, S.F. (1989): Experimental constraints on phlogopite chemistry in lamproites: 1. The effect of water activity and oxygen fugacity. *Eur. J. Mineral.*, **1**, 411-426.

Guggenheim, S. (1981): Cation ordering in lepidolite. *Am. Mineral.*, **66**, 1221-1232.

Guggenheim, S. & Bailey, S.W. (1977): The refinement of zinnwaldite-1*M* in subgroup symmetry. *Am. Mineral.*, **62**, 1158-1167.

Monier, G. & Robert, J.L. (1986): Evolution of the miscibility gap between muscovite and biotite solid solutions with increasing lithium content: an experimental study in the system K_2O-Li_2O-MgO-FeO-Al_2O_3-SiO_2-H_2O-HF at 600°C, 2 kbar PH_2O: comparison with natural lithium micas. *Mineral. Mag.*, **50**, 641-651.

Nespolo, M. & Ďurovič, S. (2002): Crystallographic basis of polytypism and twinning in micas. *Rev. Mineral. Geochem.*, A. Mottana, F.P. Sassi, J.B. Thompson, S. Guggenheim editors, **46**, 155-272.

Ni, Y. & Hughes, J.M. (1996): The crystal structure of nanpingite-2M_2, the Cs end-member of muscovite. *Am. Mineral.*, **81**, 105-110.

North, A.C.T., Phillips, D.C., Mathews, F.S. (1968): A semi-empirical method of absorption correction. *Acta Cryst.*, **A24**, 351-359.

Quensel, P. (1955): The paragenesis of the Varuträsk pegmatite including a review of its mineral assemblage. *Arkiv for Mineralogi och Geologi*, **2**, 9-125.

Raimbault, L. (1998): Composition of complex lepidolite-type granitic pegmatites and of constituent columbite-tantalite, Chèdeville, Massif Central, France. *Can. Mineral.*, **36**, 563-583.

Rieder, M., Hybler, J., Smrčok, L., Weiss, Z. (1996): Refinement of the crystal structure of zinnwaldite 2M_1. *Eur. J. Mineral.*, **8**, 1241-1248.

Sales, K.D. (1987): Atomic scattering factors for mixed atom sites. *Acta Cryst*., **A 43**, 42-44.

Sartori, F. (1976): The crystal structure of a 1*M* lepidolite. *Tscherm. Mineral. Petrogr. Mitt*., **23**, 65-75.

— (1977): The crystal structure of a 2M_1 lepidolite. *Tscherm. Mineral. Petrogr. Mitt.*, **24**, 23-37.

Sartori, F., Franzini, M., Merlino, S. (1973): Crystal structure of a 2M_2 lepidolite. *Acta Cryst.*, B **29**, 573-578.

Sheldrick, G.M. (1997): SHELX-97, program for crystal structure determination. University of Göttingen, Germany.

Siemens (1996): XSCANS: *X-ray single crystal analysis system-Technical reference.* Siemens instruments, Madison, Wisconsin, U.S.A.

Swanson, T.H. & Bailey, S.W. (1981): Re-determination of the lepidolite-2M_1 structure. *Clays Clay Miner.*, **29**, 81-90.

Takeda, H. & Burnham, C.W. (1969): Fluor-polylithionite: a lithium mica with nearly hexagonal $(Si_2O_5)^{2-}$ ring. *Miner. Journ.*, **6**, 102-109.

Takeda, H., Haga, N., Sadanaga, R. (1971): Structural investigation of a polymorphic transition between 2M_2-, 1*M*-lepidolite and 2M_1-muscovite. *Miner. Journ.*, **6**, 203-215.

Weiss, Z., Rieder, M., Smrčok, L., Petríček, V., Bailey, S.W. (1993): Refinement of the crystal structures of two "protolithionites". *Eur. J. Mineral.*, **5**, 493-502.

Zhoukhlistov, A.P., Zvyagin, B.B., Soboleva, S.V., Fedotov, A.F. (1973): The crystal structure of the dioctahedral mica 2M_2 determined by high voltage electron diffraction. *Clays Clay Miner.*, **21**, 465-470.

Received 28 July 2004
Modified version received 17 December 2004
Accepted 20 December 2004